# **Decoupled spatiotemporal patterns of avian taxonomic and functional diversity**

### **Highlights**

- Avian taxonomic (TD) and functional (FD) diversity show strong seasonal decoupling
- In the eastern US, the seasonal patterns of TD and FD are diametrically opposed
- In the western US, the seasonal signatures for TD and FD are more congruent
- Adopting an explicitly temporal framework is crucial for biodiversity analysis

#### **Authors**

Marta A. Jarzyna, James H. Stagge

#### Correspondence

jarzyna.1@osu.edu

#### In brief

Jarzyna and Stagge show that bird taxonomic diversity and functional diversity manifest decoupled seasonal patterns. This decoupling is particularly strong in the eastern US, where avian functional richness is highest in the winter despite seasonal loss of species. In the west, species and functional richness peak together during the breeding season.







### Report

# Decoupled spatiotemporal patterns of avian taxonomic and functional diversity

Marta A. Jarzyna<sup>1,2,4,\*</sup> and James H. Stagge<sup>3</sup>

- <sup>1</sup>Department of Evolution, Ecology and Organismal Biology, The Ohio State University, Columbus, OH 43210, USA
- <sup>2</sup>Translational Data Analytics Institute, The Ohio State University, Columbus, OH 43210, USA
- <sup>3</sup>Department of Civil, Environmental and Geodetic Engineering, The Ohio State University, Columbus, OH 43210, USA

<sup>4</sup>Lead contact

\*Correspondence: jarzyna.1@osu.edu https://doi.org/10.1016/j.cub.2023.01.066

#### **SUMMARY**

Each year, seasonal bird migration leads to an immense redistribution of species occurrence and abundances, 1-3 with pervasive, though unclear, consequences for patterns of multi-faceted avian diversity. Here, we uncover stark disparities in spatiotemporal variation between avian taxonomic diversity (TD) and functional diversity (FD) across the continental US. We show that the seasonality of species richness expectedly<sup>3</sup> follows a latitudinal gradient, whereas seasonality of FD instead manifests a distinct east-west gradient. In the eastern US, the temporal patterns of TD and FD are diametrically opposed. In winter, functional richness is highest despite seasonal species loss, and the remaining most abundant species are amassed in fewer regions of the functional space relative to the rest of the year, likely reflecting decreased resource availability. In contrast, temporal signatures for TD and FD are more congruent in the western US. There, both species and functional richness peak during the breeding season, and species' abundances are more regularly distributed and widely spread across the functional space than during winter. Our results suggest that migratory birds in the western US disproportionately contribute to avian FD by possessing more unique trait characteristics than resident birds, 4,5 while the primary contribution of migrants in the eastern US is through increasing the regularity of abundances within the functional space relative to the rest of the year. We anticipate that the uncovered complexity of spatiotemporal associations among measures of avian diversity will be the catalyst for adopting an explicitly temporal framework for multi-faceted biodiversity analysis.

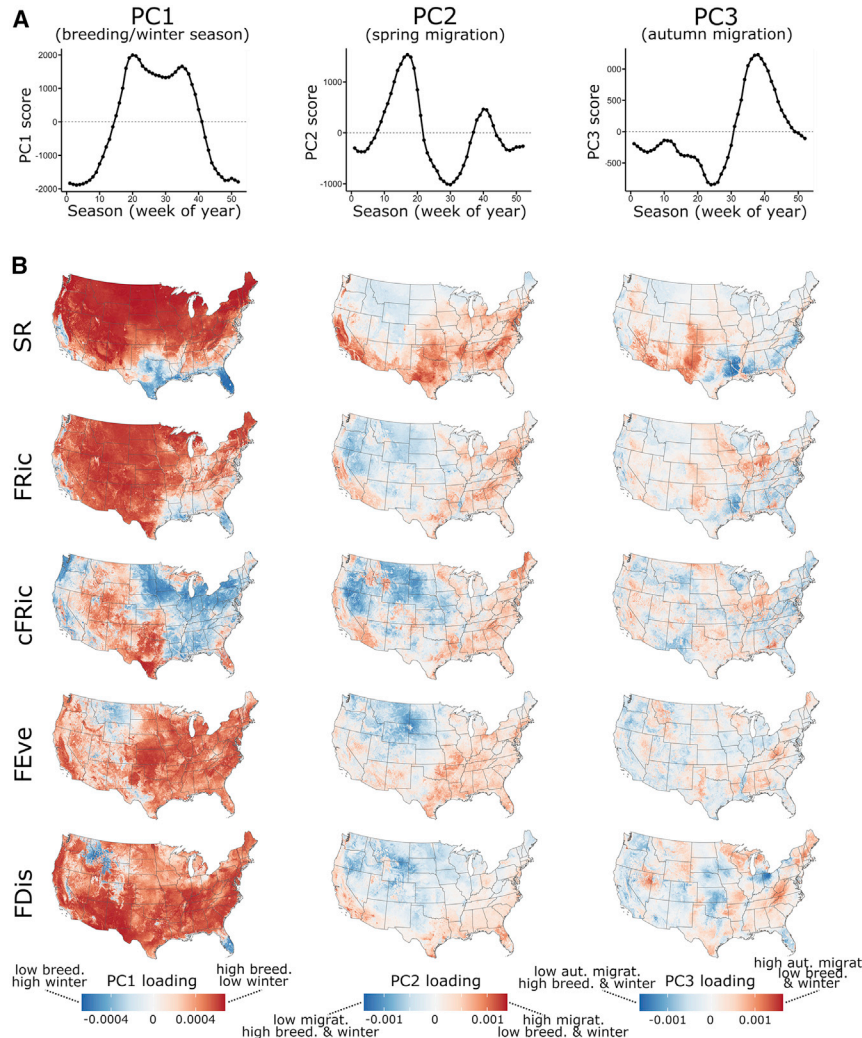
#### **RESULTS**

Pinpointing the mechanisms responsible for maintenance of biodiversity relies on accurate evaluations of biodiversity patterns, <sup>6,7</sup> but those often reflect the static conditions of one, often breeding, season<sup>8-10</sup> and ignore seasonal variability inherent in the full seasonal cycle of species. No other taxonomic group shows stronger intra-annual geographic redistribution of species occurrence and abundance than birds. Each year, billions of individuals<sup>11,12</sup> of an estimated 1,855 species (19% of all extant bird species, a percentage that strongly increases with latitude<sup>5</sup>) migrate toward lower latitudes in autumn and higher latitudes in spring in response to seasonal fluctuations in resource availability<sup>3,13,14</sup> and unfavorable weather conditions, given some species' physiological limitations. 15 These migratory movements produce seasonal patterns of biomass, abundance, and species richness (SR).3 Unexplored, however, remain the implications of the seasonal redistribution of bird occurrence and abundance for other facets of biodiversity such as functional diversity (FD), the diversity and distribution of functional traits within an assemblage of species. 16-18 FD is vital for understanding community assembly, <sup>19,20</sup> niche packing and expansion, <sup>21,22</sup> ecosystem functioning, services, stability, 23,24 and conservation prioritization.<sup>25-27</sup>

Seasonality of avian FD is likely to deviate from that of taxonomic diversity (TD) because migratory and resident birds often present different trait characteristics such as body mass<sup>28,29</sup> or clutch size.30 Migrants also often show stronger habitat31,32 (but see Reif et al.33), diet,34,35 and climate36 (but see Dufour et al.<sup>37</sup>) specialization than partial migrants or resident species, who are often generalists that possess a broader spectrum of trait values conferring tolerance to harsh winter conditions of temperate regions. Such disproportionate redistribution of trait characteristics likely leads to decoupling of avian functional from taxonomic diversity, but the spatiotemporal pattern, magnitude, and direction of such decoupling have not been previously elucidated. Here, we present the first broad-scale assessment of commonalities among seasonal patterns in avian TD and FD. We leverage relative abundance estimates during the full annual cycle for >600 North American bird species from eBird Status and Trends<sup>38</sup> for 2019 to quantify TD (SR). We combine these with avian trait databases<sup>39</sup> to quantify three independent and complementary components of FD-functional richness (FRic), functional evenness (FEve), and functional dispersion (FDis). 40 Because FRic is often strongly related with SR, we regressed log-transformed FRic against log-transformed SR and used residuals of this regression as SR-corrected values of FRic (cFRic). cFRic better reflects the true breadth of occupied functional







PC (PC2, 11% variance explained; Figure S2) further isolates migration (primarily, spring migration; positive score) from periods of wintering and breeding (negative score; Figure 1A). The third PC (PC3, 8% variance explained; Figure S2) further emphasizes the signal of autumn migration (positive score; Figure 1A). Each subsequent PC explains <5% of the variance and captures mostly stochastic fluctuations.

space, with positive cFRic (residuals) indicative of surplus and negative cFRic indicative of deficits in FRic, given SR of a given assemblage.  $^{41}$  This raised the total metrics considered to five, measured across the continental US at a 2.96  $\times$  2.96 km spatial resolution (for a total of n = 933,161 grid cells) and a weekly temporal resolution.

#### Spatiotemporal variation in avian TD and FD

We first identify the dominant modes of temporal variability in avian diversity using principal component analysis (PCA). PCA is a commonly used data reduction technique that can reduce complex patterns of potentially correlated variation into a small number of dominant "modes," or "components," that was recently suggested as a viable method to isolate consistent principal modes of spatiotemporal variation in biodiversity 13,42 (see STAR Methods and Figure S1 for the methodological workflow). We identify three principal components (PCs) that together explain 65% of weekly variance in the five avian diversity metrics across the continental US (Figure S2). The first PC (PC1; 47% variance explained; Figure S2) separates the breeding (positive score) from the wintering (negative score) season, with two distinct, lesser peaks likely associated with the temporary

Figure 1. Intra-annual variability in avian diversity—measured as species richness (SR), raw functional richness (FRic), species richness-corrected values of functional richness (cFRic), functional evenness (FEve), and functional dispersion (FDis)—is well captured by three primary modes (principal components [PCs])

(A) The scores (temporal seasonal patterns) are illustrated. The seasonal patterns of scores of the first mode (PC1) captures differences in avian diversity between breeding (high score) and wintering (low score) season, the second mode (PC2) separates migration (particularly, spring migration; high score) from periods of wintering and breeding (low score), and the third mode (PC3) further emphasizes the signal of autumn migration (high score).

(B) PC loading maps show how strongly, positively (red hues), or negatively (blue hues), the temporal pattern given by scores for each PC is expressed at a given location: PC1 (left column), PC2 (middle column), and PC3 (right column). The loading maps demonstrate strong and contrasting spatial variation in seasonality of each avian diversity measure. See also Figures S1 and S2.

addition of transient species during seasonal migration (Figure 1A). The second

the variance and captures mostly stochastic fluctuations, without a clear seasonal signature (Figure S2). A seasonal pattern of avian diversity can thus be largely reconstructed for each grid cell as the weighted combination of three principal modes: breeding/winter season (PC1), spring (PC2), and autumn (PC3) migration, where the weights (i.e., importance of each PC at different locations) are shown by the PC loading maps (Figure 1B). PC loading maps thus provide a spatial illustration of how strongly, positively, or negatively the temporal patterns given by PC scores (Figure 1A) are expressed at a given location, allowing assessment of commonalities among the seasonal patterns of each avian diversity measure. Strong positive PC loadings (red hues in Figure 1B) indicate that the temporal pattern given by each of the PC scores is expressed strongly in that region, while strong negative loadings (blue hues in Figure 1B) indicate that the temporal pattern is expressed strongly in the opposite direction. Loadings near zero indicate that the temporal pattern is barely expressed.

Avian diversity shows clear spatial patterns in the strength (loading) of temporal variation (score) patterns, but there are notable differences among avian diversity metrics in how these patterns are expressed (Figures 1 and 2A). Seasonality of SR

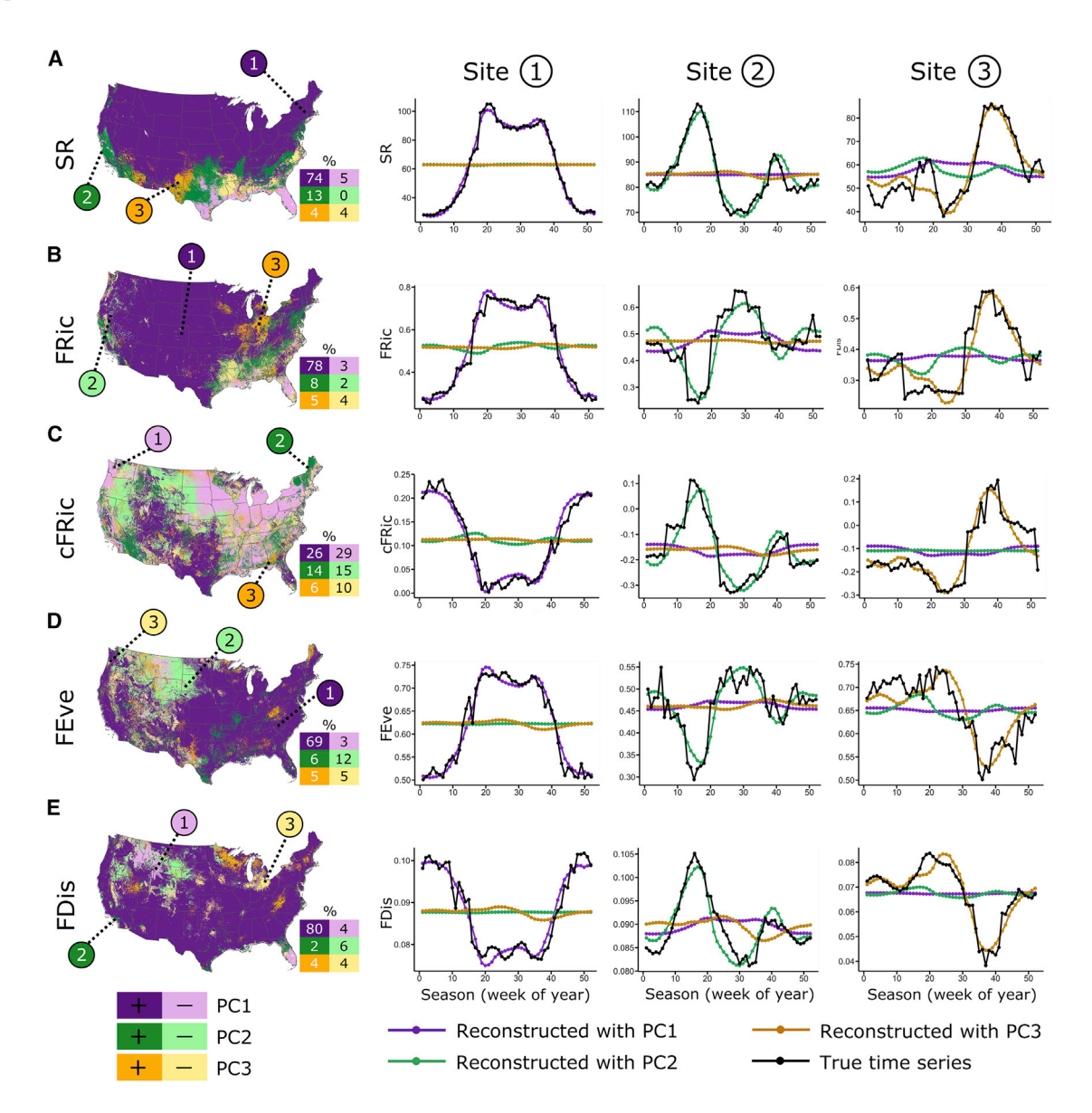


Figure 2. The ability of the first three principal components (PCs) to explain the intra-annual variability in avian diversity varies across space and among diversity metrics

Shown are the results for species richness (SR; A), raw functional richness (FRic; B), species richness-corrected values of functional richness (cFRic; C), functional evenness (FEve; D), and functional dispersion (FDis; E). We computed an empirical reconstruction of true avian diversity time series (dependent variable) as a linear model of the time series recreated by each PC's scores and loadings (independent variable; see STAR Methods for more details). The coefficient of determination, R<sup>2</sup>, of these reconstructed diversity models was used as a measure of the variation explained by each PC. In purple are regions where PC1 explains the most variation in avian diversity. In green and yellow are the regions where PC2 and PC3, respectively, explain the most variation in avian diversity. Dark and light hues indicate the positive and negative PC loadings, respectively. Inset boxes indicate the percentage of the study area falling within each category. Avian diversity at select sites (right panels) show seasonal patterns broadly consistent with those recreated by the PC that explains the most variation for that location.

demonstrates a strong latitudinal gradient, with the northern US (n = 693,160 grid cells,  $\sim$ 74% of study region) characterized by high breeding season SR and low winter SR (strongly positive PC1 loadings; Figures 1 and 2A). Along the Gulf of Mexico coast, SR instead peaks during winter (n = 48,251,  $\sim$ 5%; strongly negative PC1 loadings). Known migratory staging areas across the South, Southeast, Southwest, and California (n = 159,452,  $\sim$ 17%) experience spring and autumn peaks in SR (strongly positive PC2 and PC3 loadings; Figures 1 and 2A), with some spatial differences between PC2 (spring) and PC3 (autumn) loading. A few patches in the Southeast (n = 32,298,  $\sim$ 4%) instead experience autumn troughs in SR (Figures 1 and 2A). Raw FRic expectedly shows fairly strong spatiotemporal congruence with SR, with only small deviations for parts of Texas and the Midwest where FRic peaks during the breeding season and autumn migration, respectively (Figures 1 and 2B).



In stark contrast to the strongly correlated SR and FRic, cFRic peaks during winter across most of the East, Midwest, and Pacific coast (strongly negative PC1 loadings; n = 265,851, ~29%; Figures 1 and 2C). This temporal signature implies that the total breadth of functional space occupied by a bird assemblage is higher during winter than would be expected after accounting for seasonal declines in SR due to migration but lower during summer when migrants are back on their breeding grounds. In contrast, breeding season peaks in cFRic (strongly positive PC1 loading) are common across northern Michigan, Florida, Texas, the Rocky Mountains, and California's Central Valley (n = 240,285, ~26%; Figures 1 and 2C). For Florida and Texas in particular, this suggests that the influx of short-distance migrants from northern latitudes during winter leads to assemblage-wide declines in cFRic. Importantly, passage migrants strongly influence the seasonality of cFRic. Specifically, the high plateaus of the Intermountain West experience spring troughs in cFRic (strongly negative PC2 loadings; n = 144,797, ~15%; Figures 1 and 2C), while parts of the Southwest, Southeast, and New England see spring and autumn peaks (strongly positive PC2 and PC3 loadings;  $n = 188,824, \sim 20\%$ ; Figures 1 and 2C).

Seasonality of FEve broadly displays an east-west gradient (Figures 1 and 2D), with breeding season peaks (strongly positive PC1 loadings) common to east of the Rocky Mountains, in parts of the Great Basin, and along the Pacific coast (n = 642,027,  $\sim$ 69%; Figures 1 and 2D). Such a temporal pattern indicates a more even distribution of species' relative abundances in the functional space during the breeding season than during winter. In contrast, in winter, species' relative abundances amass in fewer regions of the functional space relative to the rest of the vear. Passage migrants influence seasonality of FEve particularly strongly in high elevation and topographically varying regions. The high plateaus of Intermountain West, parts of the Rocky Mountains, and the Sierras exhibit more irregular distribution of species' relative abundances within the functional space (low FEve) during spring (negative PC2 loadings; n = 108,813,  $\sim$ 12%) and the breeding season (negative PC1 loadings;  $n = 34,122, \sim 4\%$ ) relative to the rest of the year. Parts of the Rocky, Chisos, Ozark, and Appalachian Mountains (n = 100,862, ~11%) see FEve peak in spring and autumn relative to other seasons (Figures 1 and 2D).

Strong breeding-wintering seasonality characterizes FDis across most of the continental US (n = 745,939; ~80%; Figures 1 and 2E), with peaks typically observed during the breeding season (strongly positive PC1 loadings). This temporal signature implies that, during the breeding season, abundant species are spread further away from the centroid of the functional space relative to rare species, but in winter, they are positioned closer to the centroid. The only regions with winter relative increases in FDis (negative PC1 loadings) are the northern Rocky Mountains and lower Peninsular Florida (n = 32,980, ~4%; Figures 1 and 2E). Passage migrants strongly increase the dispersion of species' relative abundances in the functional space during spring and autumn relative to the rest of the year (strongly positive PC2 and PC3 loadings) in the Appalachian Mountains, the Great Lakes region, and upper Peninsular Florida (n = 52,619,  $\sim$ 6%) but lower it (strongly negative PC2 and PC3 loadings) in the high plateaus of Intermountain West, the Sierras, and the Midwest (n = 101,588,  $\sim$ 10%; Figures 1 and 2E).

#### Congruence in seasonality of avian TD and FD

Next, we conducted a clustering procedure to better synthesize findings from the three PCs and identify regions characterized by similar temporal patterns of avian diversity. We identify seven distinct spatiotemporal clusters (Figures 3 and S3). Broadly, clusters 1 (n = 140,846, ~15% of continental US) and 2 (n = 140,967, ~15%) represent locations where SR and FD peak during the breeding season and migration, except for cFRic, which alone declines during the breeding season (Figure 3B). Together, clusters 1 and 2 cover much of the eastern US (Figure 3A), with cluster 1 representing the higher elevation of the Appalachian region and southeastern plateaus and cluster 2 representing the low-lying plains and prairies of the Lower Great Lakes. Parts of California and the Pacific Northwest also show characteristics of clusters 1 and 2 (Figure 3A).

Cluster 3 (n = 120,658,  $\sim$ 13%) is broadly defined by breeding season peaks in avian diversity across nearly all measures and declines during winter, spring, and autumn (Figure 3B). cFRic is again an exception to this pattern as it instead peaks in spring and plummets in autumn (Figure 3B). Cluster 3 is characterized by high elevation and cold winter in forested regions of the Rocky Mountains, New England, upstate New York, and the Upper Great Lakes (Figure 3A). Cluster 4 (n = 99,342,  $\sim$ 11%) is characterized by low SR but high FD during the breeding season relative to the rest of the year (Figure 3B) and covers the southernmost and eastern regions of Texas, Florida, and inland California (Figure 3A), areas typically characterized by warm winters.

Broadly, clusters 5 (n = 190,523,  $\sim$ 21%) and 6 (n = 115,681,  $\sim$ 12%) experience peaks in avian diversity during the breeding season and troughs during winter, spring, and autumn (Figure 3B) and cover medium (cluster 5) to high (cluster 6) elevation plateaus of the western US (Figure 3A). Finally, cluster 7 (n = 123,113,  $\sim$ 13%) identifies locations where SR peaks during both the breeding and migration seasons and FD peaks in the breeding season (Figure 3B). Cluster 7 comprises mostly the deserts of the Southwest and extends into the prairies along the Front Range (Figure 3A). Remarkably, we find a close agreement between these emergent spatiotemporal clusters and most Bird Conservation Regions (BCRs; Figures 3A and 3C)-independently and qualitatively derived regions that are ecologically distinct in terms of their bird communities, habitat types, and resource management issues. 43 For example, Atlantic Northern Forests and Boreal Hardwood Transition BCRs correspond closely to cluster 3, while Peninsular Florida, Tamaulipan Brushlands, and Oaks and Prairies BCRs show close agreement with cluster 4 (Figure 3). However, a few BCRs (e.g., Northern Pacific Rainforest, Southern Rockies Colorado Plateau, or Mississippi Alluvial Valley) do not correspond to a single cluster but rather are composed of several clusters (Figure 3).

#### **DISCUSSION**

We show strong spatial and seasonal decoupling for multiple facets of avian diversity across the continental US. The seasonality of SR follows a latitudinal gradient, associated with north-south migratory movements of hundreds of bird species, corroborating findings from others.<sup>3</sup> In the northern US, SR is expectedly highest in the breeding season, but that temporal

Report



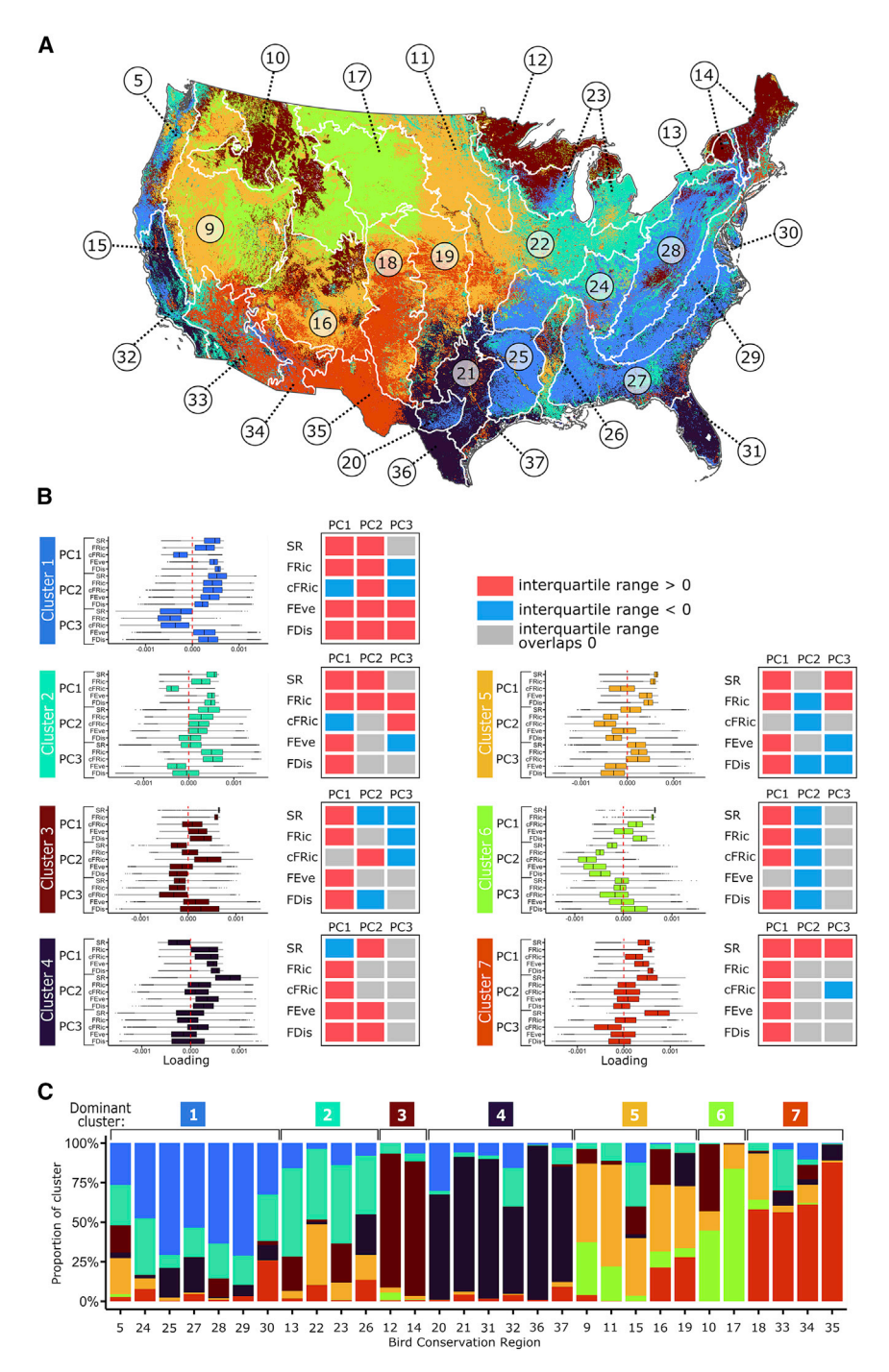


Figure 3. We identified seven unique spatiotemporal clusters that are characterized by similar temporal patterns of avian diversity (A and B) These are indicated on the map by color, unique to each cluster (A). Cluster identities are listed in (B) where the cluster color is indicated by the colored column at the left edge of each cluster's bar graph. The spatiotemporal clusters coincide strongly with the Bird Conservation Regions (BCRs), indicated by white boundaries and a numbered tag in (A). Box plots in (B) show the distribution of loadings for each principal component (PC) and each avian diversity metric (SR. species richness: FRic. raw functional richness: cFRic, species richness-corrected values of functional richness: FEve. functional evenness: FDis. functional dispersion) for locations that fall within each cluster; blue and red heat maps in (B) summarize the direction of PC loadings, with red (blue) indicating those loadings/avian diversity metric combinations whose interquartile range is positive (negative) and does not overlap zero and gray indicating that the interquartile range overlaps zero.

(C) Bar graphs show proportion of each cluster falling within each BCR. BCRs in (A) follow numbering consistent with their official designation<sup>43</sup> and are as follows: (5) Northern Pacific Rainforest, (9) Great Basin, (10) Northern Rockies, (11) Prairie Potholes, (12) Boreal Hardwood Transition, (13) Lower Great Lakes/St. Lawrence Plain, (14) Atlantic Northern Forests, (15) Sierra Nevada, (16) Southern Rockies Colorado Plateau, (17) Badlands and Prairies, (18) Shortgrass Prairie, (19) Central Mixed Grass Prairie, (20) Edwards Plateau. (21) Oaks and Prairies, (22) Eastern Tallgrass Prairie, (23) Prairie Hardwood Transition, (24) Central Hardwoods, (25) West Gulf Coastal Plain/ Ouachitas, (26) Mississippi Alluvial Valley, (27) Southeastern Coastal Plain, (28) Appalachian Mountains, (29) Piedmont, (30) New England/ MidAtlantic Coasts, (31) Peninsular Florida, (32) Coastal California, (33) Sonoran and Mojave Deserts, (34) Sierra Madre Occidental, (35) Chihuahuan Desert, (36) Tamaulipan Brushlands, and (37) Gulf Coastal Prairie.

See also Figures S1 and S3.

pattern reverses along the Gulf of Mexico coast, where SR instead peaks in winter, likely driven by seasonal influx of short-distance migrants into these wintering grounds.<sup>3</sup> Across the South, Southeast, Southwest, and California, migrants further contribute strongly to spring and autumn peaks in SR, with spatial differences between spring and autumn patterns potentially indicative of loop migration.<sup>44</sup>

The seasonality of FD manifests a more complex spatial variation, characterized by a stronger east-west gradient, further latitudinal variation superimposed on it, and some apparent

topographical effect. The diametrically opposed temporal patterns of TD and FD are most apparent in the eastern US. There, bird assemblages in the breeding season, relative to winter, are

characterized by a tightly packed functional space that leads to lower overall cFRic, a more even distribution of species' relative abundances in that space, and a wider spread of abundant species in relation to the space centroid. Such a pattern suggests a more effective use of the entire range of resources, whose availability increases during the summer months, despite the lower overall cFRic of bird assemblages. During winter, cFRic increases despite species loss, suggesting that resident birds contribute disproportionately to the breadth of the functional space occupied by bird assemblages. The





remaining most abundant species, however, are confined to fewer regions of the functional space than during the breeding season, which are likely associated with the limited resources available during winter. Likewise, along the Gulf of Mexico, multi-faceted FD peaks during the breeding season despite declines in SR, again suggesting that short-distance migrants do not significantly expand the functional breadth of bird assemblages while wintering in that region.

Across the western US, discrepancies in temporal signatures of avian diversity measures are somewhat less pronounced. Therefore, bird assemblages during the breeding season are characterized by high cFRic and a more regular, relative to winter, distribution with a wide spread of species' relative abundances in the functional space. Superimposed onto this broad pattern is a latitudinal gradient that reveals the importance of passage migrants, wherein more northerly regions are increasingly characterized by spring and autumn declines in avian diversity. This might partly result from the differential timing of migration, wherein northerly latitudes see earlier departure (in autumn) and later arrival (in spring) dates than southerly regions. Additionally, birds across the western US are known to travel shorter distances as they often combine elevational with latitudinal migration movements, a direct result of high topographic relief,46 which might ultimately lead to a more pronounced north-south gradient.

Stark differences in seasonality of cFRic suggest differential contributions of migratory and resident birds to FD across the east-west gradient. In the western US, migratory birds seemingly play a more important role in maintaining FD by contributing unique trait characteristics outside the trait spectrum represented by resident species. Indeed, dietary and habitat specializations are higher in the western US than in the east4 and narrow-ranged area, and thus, potentially more specialized, 47,48 migratory birds make up a greater proportion of avian communities in the western US.5 For example, of 15 species of hummingbirds found in the US, only the ruby-throated hummingbird (Archilochus colubris) breeds in the eastern US and is additionally considered a niche generalist compared with hummingbirds of the western US. A seasonal loss of these and other functionally unique species is likely to have an outsized effect on assemblage FD, particularly cFRic. In the eastern US, higher levels of generalization in resident birds<sup>4</sup> ensure that most regions of the functional space remain occupied during winter, albeit scarcely. Therefore, the primary contribution of migratory birds to FD is through increasing the evenness and dispersion of relative abundances within the functional space compared with the rest of the year, which ensures a high degree of niche differentiation and thus a more efficient resource use.40,45

Whether other taxonomic groups with highly seasonal life cycles show similar seasonal decoupling in TD and FD remains untested. For example, in contrast to birds, mammalian SR is highest in the western US but their FD peaks in the eastern US.<sup>49</sup> This might suggest that mammals show the reverse spatiotemporal pattern to those shown by birds, although the crucial piece of information—i.e., whether hibernating or migratory mammal species are more or less functionally unique than year-round residents and whether this varies spatially—has not yet been assessed.

The uncovered complexity of spatiotemporal associations among the different facets of avian diversity illustrates the importance of isolating unique seasonal signals of biodiversity. Our findings, paired with evidence for strong temporal non-stationarity of the effects of environmental drivers on biodiversity <sup>50,51</sup> and seasonally varying projections of regional climate change, <sup>52–55</sup> reinforce the pressing need to place the investigations of spatial patterns of biodiversity in an explicitly temporal context to ensure sound forecasting, conservation, and management of biodiversity.

#### **STAR**\*METHODS

Detailed methods are provided in the online version of this paper and include the following:

- KEY RESOURCES TABLE
- RESOURCE AVAILABILITY
  - Lead contact
  - Materials availability
  - Data and code availability
- EXPERIMENTAL MODEL AND SUBJECT DETAILS
- METHOD DETAILS
  - Species distributions and relative abundances
- QUANTIFICATION AND STATISTICAL ANALYSIS
  - Avian taxonomic and functional diversity
  - O Species richness-controlled avian functional diversity
  - O Spatiotemporal variation in avian diversity
  - Spatial congruence in seasonality of avian taxonomic and functional diversity

#### SUPPLEMENTAL INFORMATION

Supplemental information can be found online at https://doi.org/10.1016/j.cub.2023.01.066.

#### **ACKNOWLEDGMENTS**

The authors acknowledge support from the NSF DEB 1926598 to M.A.J. and NSF P2C2 2002539 to J.H.S. The work was also supported by the Byrd Polar and Climate Research Center at The Ohio State University. We thank Gil Bohrer, Sean Williams, the members of the Carstens lab, and three anonymous reviewers for feedback on earlier versions of this manuscript. We also thank Daniel Fink for valuable advice on using eBird Status and Trends data. We thank Michael Broe for his help with supercomputing and the Ohio Supercomputer Center for their computational resources, as well as thousands of volunteers who participated in eBird.

#### **AUTHOR CONTRIBUTIONS**

M.A.J. conceived the idea and M.A.J. and J.H.S. conducted all analyses and wrote the paper.

#### **DECLARATION OF INTERESTS**

The authors declare no competing interests.

Received: October 8, 2022 Revised: December 27, 2022 Accepted: January 30, 2023 Published: February 22, 2023

## Report



#### REFERENCES

- 1. Marra, P.P., Cohen, E.B., Loss, S.R., Rutter, J.E., and Tonra, C.M. (2015). A call for full annual cycle research in animal ecology. Biol. Lett. 11, 20150552. https://doi.org/10.1098/rsbl.2015.0552.
- 2. Briedis, M., Bauer, S., Adamík, P., Alves, J.A., Costa, J.S., Emmenegger, T., Gustafsson, L., Koleček, J., Krist, M., Liechti, F., et al. (2020). Broadscale patterns of the Afro-Palaearctic landbird migration. Glob. Ecol. Biogeogr. 29, 722-735. https://doi.org/10.1111/geb.13063.
- 3. Ng, W.H., Fink, D., La Sorte, F.A., Auer, T., Hochachka, W.M., Johnston, A., and Dokter, A.M. (2022). Continental-scale biomass redistribution by migratory birds in response to seasonal variation in productivity. Glob. Ecol. Biogeogr. 31, 727-739. https://doi.org/10. 1111/geb.13460.
- 4. Belmaker, J., Sekercioglu, C.H., and Jetz, W. (2012). Global patterns of specialization and coexistence in bird assemblages. J. Biogeogr. 39, 193-203. https://doi.org/10.1111/j.1365-2699.2011.02591.x.
- 5. Somveille, M., Manica, A., Butchart, S.H.M., and Rodrigues, A.S.L. (2013). Mapping global diversity patterns for migratory birds. PLoS One 8, e70907. https://doi.org/10.1371/journal.pone.0070907.
- 6. Jetz, W., McGeoch, M.A., Guralnick, R., Ferrier, S., Beck, J., Costello, M.J., Fernandez, M., Geller, G.N., Keil, P., Merow, C., et al. (2019). Essential biodiversity variables for mapping and monitoring species populations. Nat. Ecol. Evol. 3, 539-551. https://doi.org/10.1038/s41559-019-
- 7. Pereira, H.M., Ferrier, S., Walters, M., Geller, G.N., Jongman, R.H.G., Scholes, R.J., Bruford, M.W., Brummitt, N., Butchart, S.H.M., Cardoso, A.C., et al. (2013). Ecology. Essential biodiversity variables. Science 339, 277-278. https://doi.org/10.1126/science.1229931.
- 8. Hughes, E.C., Edwards, D.P., Bright, J.A., Capp, E.J.R., Cooney, C.R., Varley, Z.K., and Thomas, G.H. (2022). Global biogeographic patterns of avian morphological diversity. Ecol. Lett. 25, 598-610. https://doi.org/
- 9. Jarzyna, M.A., Quintero, I., and Jetz, W. (2021). Global functional and phylogenetic structure of avian assemblages across elevation and latitude. Ecol. Lett. 24, 196-207. https://doi.org/10.1111/ele.13631.
- 10. Callaghan, C.T., Nakagawa, S., and Cornwell, W.K. (2021). Global abundance estimates for 9.700 bird species. Proc. Natl. Acad. Sci. USA 118. e2023170118, https://doi.org/10.1073/pnas.2023170118.
- 11. Dokter, A.M., Farnsworth, A., Fink, D., Ruiz-Gutierrez, V., Hochachka, W.M., La Sorte, F.A., Robinson, O.J., Rosenberg, K.V., and Kelling, S. (2018), Seasonal abundance and survival of North America's migratory avifauna determined by weather radar. Nat. Ecol. Evol. 2, 1603-1609. https://doi.org/10.1038/s41559-018-0666-4.
- 12. Hahn, S., Bauer, S., and Liechti, F. (2009). The natural link between Europe and Africa - 2.1 billion birds on migration. Oikos 118, 624-626. https://doi. org/10.1111/j.1600-0706.2008.17309.x.
- 13. Strong, C., Zuckerberg, B., Betancourt, J.L., and Koenig, W.D. (2015). Climatic dipoles drive two principal modes of North American boreal bird irruption. Proc. Natl. Acad. Sci. USA 112, E2795-E2802.
- 14. Thorup, K., Tøttrup, A.P., Willemoes, M., Klaassen, R.H.G., Strandberg, R., Vega, M.L., Dasari, H.P., Araújo, M.B., Wikelski, M., and Rahbek, C. (2017). Resource tracking within and across continents in long-distance bird migrants. Sci. Adv. 3, e1601360. https://doi.org/10.1126/sciadv.
- 15. Pfeifer, R., Stadler, J., and Roland, B. (2017). Is the seasonal variation of abundance and species richness in birds explained by energy availability? Acta Ornithol. 52, 167-178. https://doi.org/10.3161/00016454AO2017.52.
- 16. Cardoso, P., Rigal, F., Borges, P.A.V., and Carvalho, J.C. (2014). A new frontier in biodiversity inventory: a proposal for estimators of phylogenetic and functional diversity. Methods Ecol. Evol. 5, 452-461. https://doi.org/ 10.1111/2041-210X.12173.

- 17. Gagic, V., Bartomeus, I., Jonsson, T., Taylor, A., Winqvist, C., Fischer, C., Slade, E.M., Steffan-Dewenter, I., Emmerson, M., Potts, S.G., et al. (2015). Functional identity and diversity of animals predict ecosystem functioning better than species-based indices. Proc. Biol. Sci. 282, 20142620. https:// doi.org/10.1098/rspb.2014.2620.
- 18. Safi, K., Cianciaruso, M.V., Loyola, R.D., Brito, D., Armour-Marshall, K., and Diniz-Filho, J.A.F. (2011). Understanding global patterns of mammalian functional and phylogenetic diversity. Phil. Trans. R. Soc. B 366, 2536-2544. https://doi.org/10.1098/rstb.2011.0024.
- 19. Cavender-Bares, J., Kozak, K.H., Fine, P.V.A., and Kembel, S.W. (2009). The merging of community ecology and phylogenetic biology. Ecol. Lett. 12, 693-715. https://doi.org/10.1111/j.1461-0248.2009.01314.x.
- 20. Kraft, N.J.B., Adler, P.B., Godoy, O., James, E.C., Fuller, S., and Levine, J.M. (2015). Community assembly, coexistence and the environmental filtering metaphor. Funct. Ecol. 29, 592-599. https://doi.org/10.1111/ 1365-2435.12345.
- 21. Pellissier, V., Barnagaud, J.Y., Kissling, W.D., Şekercioğlu, Ç., and Svenning, J.C. (2018). Niche packing and expansion account for species richness-productivity relationships in global bird assemblages. Glob. Ecol. Biogeogr. 27, 604-615. https://doi.org/10.1111/geb.12723.
- 22. Pigot, A.L., Trisos, C.H., and Tobias, J.A. (2016). Functional traits reveal the expansion and packing of ecological niche space underlying an elevational diversity gradient in passerine birds. Proc. Biol. Sci. 283, 20152013. https://doi.org/10.1098/rspb.2015.2013.
- 23. Cadotte, M.W., Carscadden, K., and Mirotchnick, N. (2011). Beyond species: functional diversity and the maintenance of ecological processes and services. J. Appl. Ecol. 48, 1079-1087. https://doi.org/10.1111/j.1365-2664.2011.02048.x.
- 24. Jarzyna, M.A., Norman, K.E.A., LaMontagne, J.M., Helmus, M.R., Li, D., Parker, S.M., Perez Rocha, M., Record, S., Sokol, E.R., Zarnetske, P.L., and Surasinghe, T.D. (2022). Community stability is related to animal diversity change. Ecosphere 13, e3970. https://doi.org/10.1002/ecs2.3970.
- 25. Mazel, F., Pennell, M.W., Cadotte, M.W., Diaz, S., Dalla Riva, G.V., Grenyer, R., Leprieur, F., Mooers, A.O., Mouillot, D., Tucker, C.M., and Pearse, W.D. (2018). Prioritizing phylogenetic diversity captures functional diversity unreliably. Nat. Commun. 9, 2888. https://doi.org/10.1038/ s41467-018-05126-3
- 26. Pollock, L.J., Thuiller, W., and Jetz, W. (2017). Large conservation gains possible for global biodiversity facets. Nature 546, 141-144. https://doi. org/10.1038/nature22368.
- 27. Thuiller, W., Maiorano, L., Mazel, F., Guilhaumon, F., Ficetola, G.F., Lavergne, S., Renaud, J., Roquet, C., and Mouillot, D. (2015). Conserving the functional and phylogenetic trees of life of European tetrapods. Philos. Trans. R. Soc. Lond. B Biol. Sci. 370, 20140005. https://doi. org/10.1098/rstb.2014.0005.
- 28. Hein, A.M., Hou, C., and Gillooly, J.F. (2012). Energetic and biomechanical constraints on animal migration distance. Ecol. Lett. 15, 104-110. https:// doi.org/10.1111/j.1461-0248.2011.01714.x.
- 29. Soriano-Redondo, A., Gutiérrez, J.S., Hodgson, D., and Bearhop, S. (2020). Migrant birds and mammals live faster than residents. Nat. Commun. 11, 5719. https://doi.org/10.1038/s41467-020-19256-0.
- 30. Jetz, W., Sekercioglu, C.H., and Böhning-Gaese, K. (2008). The worldwide variation in avian clutch size across species and space. PLoS Biol. 6, 2650-2657.
- 31. Martin, A.E., and Fahrig, L. (2018). Habitat specialist birds disperse farther and are more migratory than habitat generalist birds. Ecology 99, 2058-2066. https://doi.org/10.1002/ecy.2428.
- 32. Zurell, D., Gallien, L., Graham, C.H., and Zimmermann, N.E. (2018). Do long-distance migratory birds track their niche through seasons? J. Biogeogr. 45, 1459-1468. https://doi.org/10.1111/jbi.13351.
- 33. Reif, J., Hořák, D., Krištín, A., Kopsová, L., and Devictor, V. (2016). Linking habitat specialization with species' traits in European birds. Oikos 125, 405-413. https://doi.org/10.1111/oik.02276.



- Boyle, W.A., Conway, C.J., and Bronstein, J.L. (2011). Why do some, but not all, tropical birds migrate? A comparative study of diet breadth and fruit preference. Evol. Ecol. 25, 219–236. https://doi.org/10.1007/s10682-010-9403-4.
- 35. Fristoe, T.S. (2015). Energy use by migrants and residents in North American breeding bird communities. Glob. Ecol. Biogeogr. 24, 406–415. https://doi.org/10.1111/geb.12262.
- Gómez, C., Tenorio, E.A., Montoya, P., and Cadena, C.D. (2016). Niche-tracking migrants and niche-switching residents: evolution of climatic niches in New World warblers (Parulidae). Proc. Biol. Sci. 283, 20152458. https://doi.org/10.1098/rspb.2015.2458.
- Dufour, P., Descamps, S., Chantepie, S., Renaud, J., Guéguen, M., Schiffers, K., Thuiller, W., and Lavergne, S. (2020). Reconstructing the geographic and climatic origins of long-distance bird migrations.
   J. Biogeogr. 47, 155–166. https://doi.org/10.1111/jbi.13700.
- Fink, D., Auer, T., Johnston, A., Strimas-Mackey, M., Robinson, O., Ligocki, S., Hochachka, W., Jaromczyk, L., Wood, C., Davies, I., et al. (2021). eBird Status and Trends (Cornell Lab of Ornithology).
- Wilman, H., Belmaker, J., Simpson, J., de la Rosa, C., Rivadeneira, M.M., and Jetz, W. (2014). EltonTraits 1.0: species-level foraging attributes of the world's birds and mammals. Ecology 95, 2027. https://doi.org/10.1890/ 13-1917 1
- Villéger, S., Mason, N.W.H., and Mouillot, D. (2008). New multidimensional functional diversity indices for a multifaceted framework in functional ecology. Ecology 89, 2290–2301.
- Gaüzère, P., O'Connor, L., Botella, C., Poggiato, G., Münkemüller, T., Pollock, L.J., Brose, U., Maiorano, L., Harfoot, M., and Thuiller, W. (2022). The diversity of biotic interactions complements functional and phylogenetic facets of biodiversity. Curr. Biol. 32, 2093–2100.e3. https:// doi.org/10.1016/j.cub.2022.03.009.
- Zuckerberg, B., Strong, C., LaMontagne, J.M., St George, S., Betancourt, J.L., and Koenig, W.D. (2020). Climate dipoles as continental drivers of plant and animal populations. Trends Ecol. Evol. 35, 440–453. https:// doi.org/10.1016/j.tree.2020.01.010.
- 43. Babcock, K., Baxter, C., Brown, S., Ford, B., Johnson, R., Leach, J., McCauley, J., Myers, G., Omernik, J., Pashley, D., et al. (1998). A proposed framework for delineating ecologically-based planning, implementation, and evaluation units for cooperative bird conservation in the U.S. (U.S. Fish and Wildlife Service).
- 44. La Sorte, F.A., Fink, D., Hochachka, W.M., Farnsworth, A., Rodewald, A.D., Rosenberg, K.V., Sullivan, B.L., Winkler, D.W., Wood, C., and Kelling, S. (2014). The role of atmospheric conditions in the seasonal dynamics of North American migration flyways. J. Biogeogr. 41, 1685–1696. https://doi.org/10.1111/jbi.12328.
- Mason, N.W.H., Mouillot, D., Lee, W.G., and Wilson, J.B. (2005). Functional richness, functional evenness and functional divergence: the primary components of functional diversity. Oikos 111, 112–118. https:// doi.org/10.1111/j.0030-1299.2005.13886.x.
- Boyle, W.A. (2017). Altitudinal bird migration in North America. Auk 134, 443–465.
- Botts, E.A., Erasmus, B.F.N., and Alexander, G.J. (2013). Small range size and narrow niche breadth predict range contractions in South African frogs. Glob. Ecol. Biogeogr. 22, 567–576. https://doi.org/10.1111/geb. 12027.
- Slatyer, R.A., Hirst, M., and Sexton, J.P. (2013). Niche breadth predicts geographical range size: a general ecological pattern. Ecol. Lett. 16, 1104–1114. https://doi.org/10.1111/ele.12140.
- Oliveira, B.F., Machac, A., Costa, G.C., Brooks, T.M., Davidson, A.D., Rondinini, C., and Graham, C.H. (2016). Species and functional diversity accumulate differently in mammals. Glob. Ecol. Biogeogr. 25, 1119– 1130. https://doi.org/10.1111/geb.12471.
- Wolkovich, E.M., Cook, B.I., McLauchlan, K.K., and Davies, T.J. (2014).
  Temporal ecology in the Anthropocene. Ecol. Lett. 17, 1365–1379. https://doi.org/10.1111/ele.12353.

- Zuckerberg, B., Fink, D., La Sorte, F.A., Hochachka, W.M., and Kelling, S. (2016). Novel seasonal land cover associations for eastern North American forest birds identified through dynamic species distribution modelling. Divers. Distrib. 22, 717–730. https://doi.org/10.1111/ddi. 12428.
- Dunn, R.J.H., Alexander, L.V., Donat, M.G., Zhang, X., Bador, M., Herold, N., Lippmann, T., Allan, R., Aguilar, E., Barry, A.A., et al. (2020).
  Development of an updated global land in situ-based data set of temperature and precipitation extremes: HadEX3. J. Geophys. Res. Atmos. 125. e2019JD032263. https://doi.org/10.1029/2019JD032263.
- Abatzoglou, J.T., and Redmond, K.T. (2007). Asymmetry between trends in spring and autumn temperature and circulation regimes over western North America. Geophys. Res. Lett. 34, 5. https://doi.org/10.1029/ 2007GL030891.
- Pendergrass, A.G., Knutti, R., Lehner, F., Deser, C., and Sanderson, B.M. (2017). Precipitation variability increases in a warmer climate. Sci. Rep. 7, 17966. https://doi.org/10.1038/s41598-017-17966-y.
- Wuebbles, D., Meehl, G., Hayhoe, K., Karl, T.R., Kunkel, K., Santer, B., Wehner, M., Colle, B., Fischer, E.M., Fu, R., et al. (2014). CMIP5 climate model analyses: climate extremes in the United States. Bull. Amer. Meteor. Soc. 95, 571–583. https://doi.org/10.1175/BAMS-D-12-00172.1.
- Laliberté, E., Legendre, P., and Shipley, B. (2014). FD: measuring functional diversity (FD) from multiple traits, and other tools for functional ecology. R package version 1.0-12.
- de Bello, F., Botta-Dukát, Z., Lepš, J., and Fibich, P. (2021). gawdis: Multi-trait dissimilarity with more uniform contributions. R package version 0.1.2
- Fink, D., Damoulas, T., and Dave, J. (2013). Adaptive spatio-temporal exploratory models hemisphere-wide species distributions from massively crowdsourced eBird data. In Twenty-Seventh AAAI Conference on Artificial Intelligence (AAAI-13).
- Fink, D., Auer, T., Johnston, A., Ruiz-Gutierrez, V., Hochachka, W.M., and Kelling, S. (2020). Modeling avian full annual cycle distribution and population trends with citizen science data. Ecol. Appl. 30, e02056. https://doi. org/10.1002/eap.2056.
- Kissling, W.D., Sekercioglu, C.H., and Jetz, W. (2012). Bird dietary guild richness across latitudes, environments and biogeographic regions. Glob. Ecol. Biogeogr. 21, 328–340. https://doi.org/10.1111/j.1466-8238. 2011.00679.x.
- Junker, R.R., Lechleitner, M.H., Kuppler, J., and Ohler, L.M. (2019). Interconnectedness of the Grinnellian and Eltonian niche in regional and local plant-pollinator communities. Front. Plant Sci. 10, 1371. https://doi. org/10.3389/fpls.2019.01371.
- Pavoine, S., Vallet, J., Dufour, A.-B., Gachet, S., and Daniel, H. (2009). On the challenge of treating various types of variables: application for improving the measurement of functional diversity. Oikos 118, 391–402. https://doi.org/10.1111/j.1600-0706.2008.16668.x.
- de Bello, F., Botta-Dukát, Z., Lepš, J., and Fibich, P. (2021). Towards a more balanced combination of multiple traits when computing functional differences between species. Methods Ecol. Evol. 12, 443–448. https:// doi.org/10.1111/2041-210X.13537.
- 64. Palacio, F.X., Callaghan, C.T., Cardoso, P., Hudgins, E.J., Jarzyna, M.A., Ottaviani, G., Riva, F., Graco-Roza, C., Shirey, V., and Mammola, S. (2022). A protocol for reproducible functional diversity analyses. Ecography 2022, e06287. https://doi.org/10.1111/ecog.06287.
- Mammola, S., Carmona, C.P., Guillerme, T., and Cardoso, P. (2021).
  Concepts and applications in functional diversity. Funct. Ecol. 35, 1869–1885. https://doi.org/10.1111/1365-2435.13882.
- Blonder, B., Lamanna, C., Violle, C., and Enquist, B.J. (2014). The n-dimensional hypervolume. Glob. Ecol. Biogeogr. 23, 595–609. https:// doi.org/10.1111/geb.12146.
- Villéger, S., Ramos Miranda, J., Flores Hernández, D., and Mouillot, D. (2010). Contrasting changes in taxonomic vs. functional diversity of

## **Report**



- tropical fish communities after habitat degradation. Ecol. Appl. 20, 1512-1522. https://doi.org/10.1890/09-1310.1.
- 68. Laliberté, E., and Legendre, P. (2010). A distance-based framework for measuring functional diversity from multiple traits. Ecology 91, 299-305. https://doi.org/10.1890/08-2244.1.
- 69. Botta-Dukát, Z. (2005). Rao's quadratic entropy as a measure of functional diversity based on multiple traits. J. Veg. Sci. 16, 533-540. https://doi.org/ 10.1111/j.1654-1103.2005.tb02393.x.
- 70. Zupan, L., Cabeza, M., Maiorano, L., Roquet, C., Devictor, V., Lavergne, S., Mouillot, D., Mouquet, N., Renaud, J., and Thuiller, W. (2014). Spatial mismatch of phylogenetic diversity across three vertebrate groups and
- protected areas in Europe. Divers. Distrib. 20, 674-685. https://doi.org/ 10.1111/ddi.12186.
- 71. Swenson, N.G. (2011). Phylogenetic beta diversity metrics, trait evolution and inferring the functional beta diversity of communities. PLoS One 6, e21264. https://doi.org/10.1371/journal.pone.0021264.
- 72. Jarzyna, M.A., and Jetz, W. (2018). Taxonomic and functional diversity change is scale dependent. Nat. Commun. 9, 2565. https://doi.org/10. 1038/s41467-018-04889-z.
- 73. Jarzyna, M.A., and Stagge, J.H. (in review). Principal component analysis to assess biodiversity change.





#### **STAR**\*METHODS

#### **KEY RESOURCES TABLE**

REAGENT or RESOURCE	SOURCE	IDENTIFIER
Deposited data		
eBird Status & Trends	Fink et al. <sup>38</sup>	N/A
EltonTraits 1.0	Wilman et al.39	N/A
Software and algorithms		
R package FD	Laliberté et al. <sup>56</sup>	https://uribo.github.io/rpkg_showcase/data-analysis/FD.html
R package gawdis	de Bello et al.57	https://rdrr.io/cran/gawdis/src/R/gawdis.R
R code used to perform analyses of this paper	N/A	https://doi.org/10.5281/zenodo.7412405

#### **RESOURCE AVAILABILITY**

#### **Lead contact**

Further information and requests for resources and reagents should be directed to and will be fulfilled by the lead contact, Marta A. Jarzyna (jarzyna.1@osu.edu).

#### **Materials availability**

This study did not generate new unique materials.

#### Data and code availability

All data used in this paper are from published or downloadable online sources. See key resources table for links toward the basal data. The code used to run analyses is available on GitHub and archived with zenodo; DOIs are listed in the key resources table.

#### **EXPERIMENTAL MODEL AND SUBJECT DETAILS**

We used data from eBird Status and Trends (S&Ts) published by the Cornell Lab of Ornithology.<sup>38</sup> eBird S&Ts provide modeled estimates of weekly species occurrence and relative abundance for 807 species. We used data for 2019 (data version 2020, released in 2021<sup>38</sup>).

#### **METHOD DETAILS**

#### Species distributions and relative abundances

We used bird species occurrence and relative abundance estimates from eBird Status and Trends (S&Ts) data for 2019 published by the Cornell Lab of Ornithology<sup>38</sup> (see Figure S1 for the methodological workflow). 2019 eBird S&Ts provide modeled estimates of weekly occurrence and relative abundance for 807 species. Species' occurrence and relative abundance estimates in S&Ts are obtained using the Adaptive Spatio-Temporal Exploratory Model (AdaSTEM) - i.e., an ensemble model designed to include essential information about spatial and temporal scales<sup>58</sup> and account for intra-annual variability in species distributions. AdaSTEM incorporates the following classes of predictors: observation effort predictors that account for variation in detection rates (e.g., search effort, distance traveled by observes, checklist calibration index, etc.), predictors that account for variation at different temporal scales (e.g., time of day, time of year), and environmental descriptors derived from remote-sensing data that capture associations of species with land cover, elevation, and topography.<sup>59</sup> For each species, occurrence and relative abundance predictions are made at a weekly temporal resolution and a spatial resolution of 2.96 x 2.96 km. Relative abundance in eBird S&Ts is defined as the count of individuals of a given species detected by an expert eBirder on a 1 hour, 1 kilometer traveling checklist at the optimal time of day. The relative abundance estimates from eBird S&Ts thus allow for obtaining estimates of avian diversity across North America without having to model raw eBird records. We note that even though relative abundance estimates within a species are comparable across space and time, their comparison across species is problematic. Consequently, contributions of different species to functional diversity might not be captured properly and the estimates of absolute functional diversity might be inaccurate, particularly when dealing with functional diversity indices that are abundance-based. We posit, however, that our results are robust with respect to this potential issue. This is because our primary goal is to understand the relative differences in functional diversity across seasons rather than their absolute values per se. Because the cross-species biases are the same across regions and seasons (Daniel Fink, personal communication), contributions of each species to functional diversity will also be biased in a consistent way across space and time, allowing



for robust capture of the patterns of spatiotemporal variation in avian functional diversity. eBird Status and Trends data used here were downloaded in February 2022 and reflect species relative abundance estimates of 2019 (data version 2020, released in 2021<sup>38</sup>). Data version 2021 was not available at the time of the analysis and submission.

Before quantifying bird diversity, we removed pelagic species, which are typically poorly sampled by eBird observers. To decrease the computational cost and ensure taxonomic completeness—crucial for robust estimation of assemblage composition—we truncated the data to the continental US and only included species that were recorded in the continental US during at least one week in a year. Ultimately, we included 630 bird species. We ensured that our species list is taxonomically complete by cross-checking with AviBase checklist for the contiguous US. AviBase checklist listed a total of 2,272 entries, of which 11 were extinct or extirpated species, 261 were hybrids, 534 were subspecies, 499 were observations not id'ed to the species level, 241 were rare or accidental species, and 6 were species who were either introduced (but without established populations—e.g., Red-masked Parakeet, native to Peru and Ecuador, or Northern Red Bishop from Africa) or species whose distributions were outside of the continental US and must have been either id'ed erroneously or seen accidentally in the US in the past (e.g., Pink-footed Goose, native to Eurasia, or Zenaida Dove, native to the Caribbean). None of these were included in our analysis because their very low population abundances preclude STEM modeling, and they provide negligible contributions to overall diversity. Of the remaining 720 species, 90 were pelagic seabirds. The remaining 630 species in AviBase were included in our analysis.

#### **QUANTIFICATION AND STATISTICAL ANALYSIS**

#### **Avian taxonomic and functional diversity**

We quantified species richness (SR) at a weekly temporal resolution and a spatial resolution of 2.96 km as the count of all species whose relative abundances were greater than zero.<sup>3</sup> We based estimates of all functional diversity metrics on a compilation of traits in four trait categories: body mass, diet, foraging niche, and activity time, available through EltonTraits 1.0.<sup>39</sup> We chose these traits because they reflect well species' functional roles in an ecosystem.<sup>60,61</sup> Diet and foraging niche categories included seven axes each: proportions of invertebrates, vertebrates, carrion, fruits, nectar and pollen, seeds, and other plant materials in species' diet (diet); proportional use of water below surface, water around surface, terrestrial ground level, understory, mid canopy, upper canopy, and aerial (foraging niche). Activity time included two axes: diurnal and nocturnal. We acknowledge that bird dietary characteristics might change across seasons, but currently such higher temporal resolution data are not available for most species included in this analysis.

To gain a comprehensive understanding of functional diversity of each assemblage across space and time, we first obtained a species' multivariate functional dissimilarities using corrected Gower's distance as implemented in the package 'gawdis'. <sup>57</sup> Gower's distance can handle quantitative, semi-quantitative and qualitative traits <sup>62</sup> and the corrected version of Gower's distance <sup>57</sup> additionally balances particularly well the contribution of traits (and trait groups) to overall dissimilarity, which is especially important when using highly dimensional data and fuzzy coded traits. <sup>63</sup> We optimized trait weights with the 'optimization' method for 300 iterations (the default); de Bello <sup>63</sup> showed that 300 iterations was enough to provide similar contributions of traits to multi-trait dissimilarity as the analytical solution. The optimization procedure resulted in the following weights: 0.01251063 (proportion of invertebrates), 0.07373712 (vertebrates), 0.06271028 (carrion), 0.09091175 (fruits), 0.02308233 (nectar and pollen), 0.06181708 (seeds), 0.04332023 (other plant materials), 0.03886894 (proportional use of water below surface), 0.03764052 (water around surface), 0.03472883 (terrestrial ground), 0.02036610 (understory), 0.10013602 (mid canopy), 0.04156486 (upper canopy), 0.09982529 (aerial), 0.14174089 (activity time), and 0.11703913 (body mass). The weights for the dietary category sum to 0.3680894, and weights for the foraging stratum sum to 0.3731306. Together, all weights sum to 1.

We then used the functional dissimilarity matrix to construct a trait space using a convex hull method. We chose a convex hull method to construct the trait space because it represents differences based on continuous and non-continuous traits more accurately than the dendrogram method, 40,64,65 but is less computationally intensive than the hypervolume method. 66 We then used three indices of functional diversity - functional richness (FRic), functional evenness (FEve), and functional dispersion (FDis) - to provide a comprehensive characterization of the trait space, while also being independent of one another 40,65; here, the Pearson correlation coefficient r between these three variables varied between -0.18 and 0.37, attesting to their independence from one another. FRic describes the total breadth of trait diversity present in an assemblage; FEve reflects the regularity of the distribution of species' relative abundances within the functional trait space; FDis summarizes the overall spread and distribution of species' relative abundances in an assemblage, relative to the centroid of the functional trait space. 67,68 To obtain FRic, FEve, and FDis for each week and at each 2.96 x 2.96 km grid cell, we used the 'dbFD' function in package 'FD'. 56 Specifically, FRic was calculated as the convex hull volume and based on the first three PCoA axes. 40 Reduction to three dimensions was necessary for FRic because the construction of convex hulls requires more species than traits (here represented by PCoA axes) and we used four as the lowest number of species necessary for functional diversity to be obtained. Additionally, using more than three PCoA axes was computationally not feasible. We standardized FRic by the 'global' FRic that includes all species so that it was constrained by 0 and 1 and comparable across the spatiotemporal domain. FEve was calculated as the regularity of species functional distances along the minimum spanning tree. 40 FDis was calculated as the mean distance of species to their collective centroid in functional trait space. 68 We chose FDis<sup>68</sup> instead of closely related functional divergence (FDiv)<sup>40</sup> or Rao's quadratic entropy<sup>69</sup> because it better estimates the dispersion of species in trait space. 68 Calculation of FEve and FDis was based on all PCoA axes. FDis is constrained by 0 but has no upper limit, while FEve is constrained by 0 and 1. We used the 'sqrt' correction for negative eigenvalues. Though both FEve and FDis





integrate information on species' relative abundances, we note that only cross-seasonal comparisons can be made for these two abundance-based metrics. This is because comparisons of relative abundances among species within seasons are invalid (see STAR Methods and method details).

All avian diversity indices were computed for each 2.96 x 2.96 km grid cell across the contiguous US (n=933,161 grid cells) and for each week, resulting in a total of  $\sim$  52M values per avian diversity metric. We used statistical software R v3.6.0 for all analyses and utilized Ohio Supercomputer Center (OSC) Pitzer cluster to run all calculations and models, for a total of approximately 11,000 hours of runtime.

#### Species richness-controlled avian functional diversity

Functional richness is strongly related to species richness and its interpretation benefits from statistically controlling for this association. To control for species richness, we regressed, separately for each week, log-transformed FRic against log-transformed SR using a simple linear regression and used residuals of this regression as SR-corrected values of FRic (cFRic). Residuals quantify deviations of FRic from the expectation given SR, 18,41,45,70 with positive residuals indicative of surplus and negative residuals indicative of deficits in functional richness given species richness of that assemblage. 41 While another common method to obtain SR-corrected values of functional diversity calls for a randomization procedure wherein species identities are shuffled hundreds of times, 71,72 such a procedure would require 100s of time the aforementioned run times (> 1,000,000 hours) and was not computationally feasible here. FDis and FEve are based on relative abundance and are thus independent of species richness and do not require a correction. 40,68

#### Spatiotemporal variation in avian diversity

We applied Principal Component Analysis (PCA) to identify the dominant components of temporal (here, seasonal) variation in avian diversity, find regions that are characterized by similar seasonal patterns of avian diversity, and identify commonalities in spatiotemporal signatures across the different indices of avian diversity. Below we provide a brief description of the principles of PCA in the context of analysis of biodiversity change; for a more thorough explanation we refer the reader to Jarzyna and Stagge. 73

We first created a 2-dimensional matrix  $\mathbf{Y}[t, ij]$  where each row t is a time step (i.e., week), and each column holds values of an avian diversity index, i (here, i=5: SR, FRic, cFRic, FEve, and FDis) measured at a location, i. Matrix Y is then subject to PCA, which transforms these multivariate data into a dataset measured along new orthogonal axes organized in such a way that the first axis, or Principal Component (PC), captures the largest proportion of variance in the data. The second PC (PC2) captures the second largest proportion of variance, measured orthogonally to PC1, and so on. These new PCs are orthogonal, i.e., uncorrelated with each other. Since one of the primary goals of PCA is dimensionality reduction, we typically only consider the most important PCs—i.e., those that capture a significant amount of variance in the data or are functionally important.

PCA decomposes the original matrix Y[t, ii] into two new matrices, referred to as PC loadings, U, and PC scores, V

$$Y = \mu + U V^{t} \sigma$$
 (Equation 1)

where the loading matrix **U** has dimensions equal to ij x k, or the number of measurements across all sites and indices by the number of principal components, k. The score matrix V has dimensions of t x k where t is the number of time steps. All avian diversity indices were first centered and normalized independently for each site and metric by calculating the long-term mean, µ, and standard deviation,  $\sigma$ , for each column of the original **Y** matrix.

PC scores describe the temporal expression of each PC, centered around the long-term mean, μ. In the context of our analysis, PC scores capture the dominant seasonal pattern of avian diversity. For example, a transition of PC scores from strongly negative at the beginning of the year to strongly positive in the summer and strongly negative again towards the end of the year captures breedingwinter season variation in avian diversity. PC loadings indicate how strongly, positively or negatively, the temporal pattern given by PC scores is expressed at a given location. Strong positive loadings mean that the average temporal pattern given by PC scores is expressed strongly in that region, strong negative loadings indicate the temporal pattern given by PC scores is expressed strongly in the opposite direction, and loadings near zero indicate that the temporal pattern given by PC scores is barely expressed, producing values of biodiversity near the mean during the entire time period. Loadings maps can be produced for all k PCs, with later PCs often capturing increasingly random spatial variation. Note that the true temporal pattern of avian diversity will always be a combination of the principal modes, but the stronger loadings on a given PC the stronger the effect of that particular Principal Component on avian diversity (see below); PC loadings can thus be thought of as weights indicating the contribution of each PC to the true temporal pattern.

Once we calculated the PC scores and loadings and selected the number of PCs to consider, we used subset versions of the loading and score matrices, U and V, to show the effect of each PC as well as the cumulative effect of all considered PCs together on avian diversity over time, at selected sites. To do that, we multiplied  $\bf U$  by the transpose of the score matrix,  $\bf V^t$ , to produce a matrix in 'normalized space'. Because we originally chose to normalize the data, we multiplied  $UV^t$  by the standard deviation,  $\sigma$ , and added the mean,  $\mu$ , back to obtain reconstructions of the original avian diversity metrics (Equation 2). For a single site and  $k^{th}$  PC, this becomes:

$$Div_{i,j,k}[t] = \mu_{i,j} + \sigma_{i,j} \times [U_{i,j,k} \times V_k[t]]$$
 (Equation 2)



where  $U_{i,i,k}$  is a single loading value for  $PC_k$  and a given site/avian diversity metric;  $V_k[t]$  is a score vector for  $PC_k$  which changes over time. The long-term mean and standard deviation of a avian diversity metric j at the location i are given by  $\mu_{i,i}$  ad  $\sigma_{i,i}$ , respectively. PC loadings and scores therefore work together to reconstruct the original avian diversity at each site and time step by calculating the number of standard deviations from the long-term mean. Lastly, we compared the reconstructed values of avian diversity metrics with true avian diversity time series for select locations.

We conducted Principal Component Analysis using function 'prcomp' from a package 'stats' in R.

#### Spatial congruence in seasonality of avian taxonomic and functional diversity

To assess agreement in spatiotemporal patterns of all avian diversity metrics, we first evaluated correlations among the loadings for the first three PCs (which together accounted for ca. 65% variance in the data; Figure S2) for each pair-wise association of avian diversity metrics (SR, FRic, cFRic, FEve, FDis). To further evaluate congruence in spatiotemporal variation among avian diversity metrics, we conducted a clustering procedure using k-means clustering algorithm. K-means algorithm partitions observations into k clusters in which each observation belongs to the cluster with the nearest mean in q-dimensional space, where the q axes represent the number of measurements. For this example, q = 15 because clustering was based on loading values from the five diversity metrics and three principal components. We first performed a k-means clustering procedure on a training dataset (a subset of 20,000 locations) and used a goodness-of-fit metric (silhouette width) that is based on the local maximum to select the most appropriate number of clusters (Figure S3). We then used a function 'kcca' from package 'flexclust' to partition observations into clusters with the closest k-centroid. Repeated tests with random samples produced stable cluster estimates, providing confidence in the use of a training subset rather than the full dataset.